Electronic Supplementary Material (ESI) for Physical Chemistry Chemical Physics.
This journal is © the Owner Societies 2019

Relevance of Dzyaloshinskii-Moriya spectral broadenings in promoting spin decoherence: a pulsed-EPR comparative study of two structurally related iron(III) and chromium(III) spin-triangle molecular qubits

*Jérôme Robert, Nathalie Parizel, Philippe Turek, Athanassios K. Boudalis**

Supporting Information

1. Spin-lattice relaxation

1.1. Saturation recovery studies of Fe_3

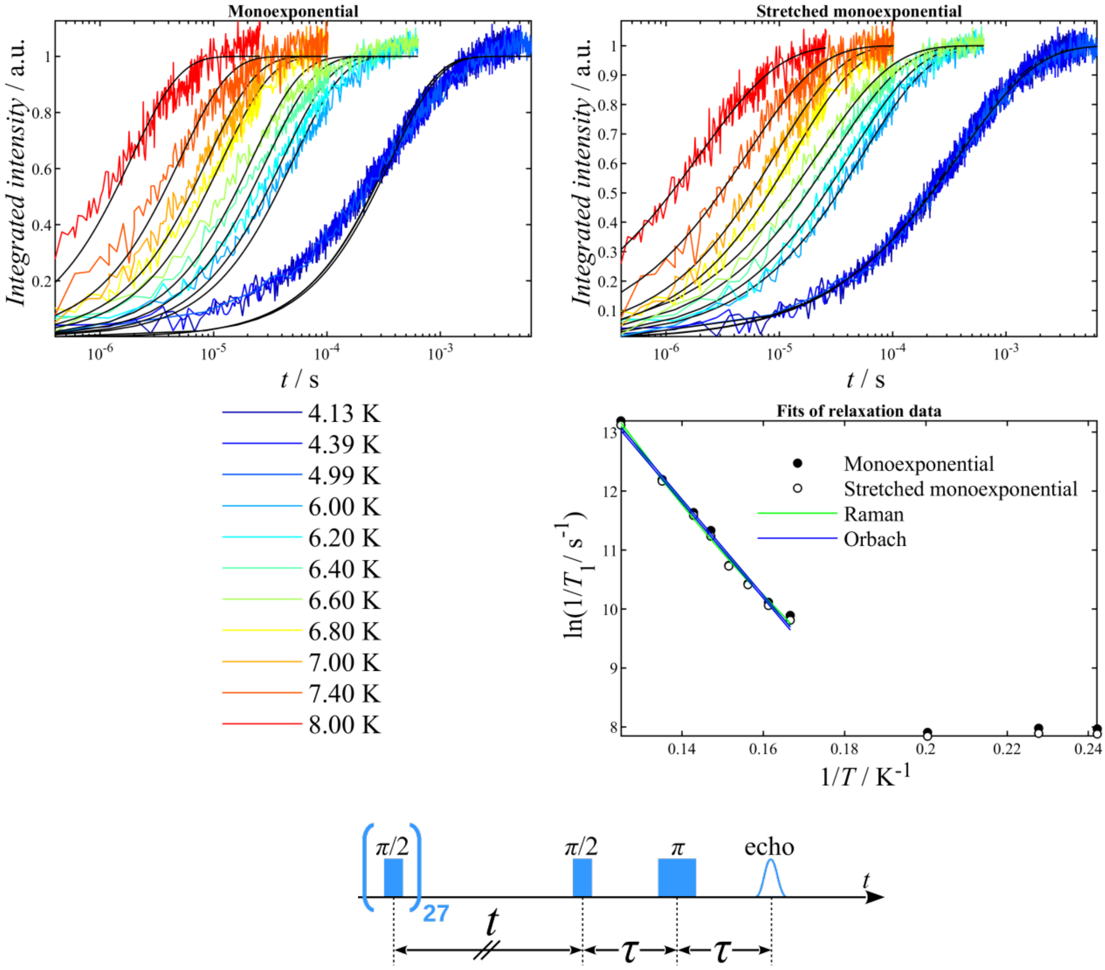

Figure S1. Variable-temperature saturation recovery data of **Fe_3** (colored lines) and fits to monoexponential (top left) and stretched exponential (top right) laws (black lines). The derived T_1 times are plotted as $1/T_1$ vs $1/T$ (bottom right) and the high-T regimes are fitted to Orbach and Raman processes. The pulse sequence is shown at the bottom.

1.2. Saturation recovery studies of Cr$_3$

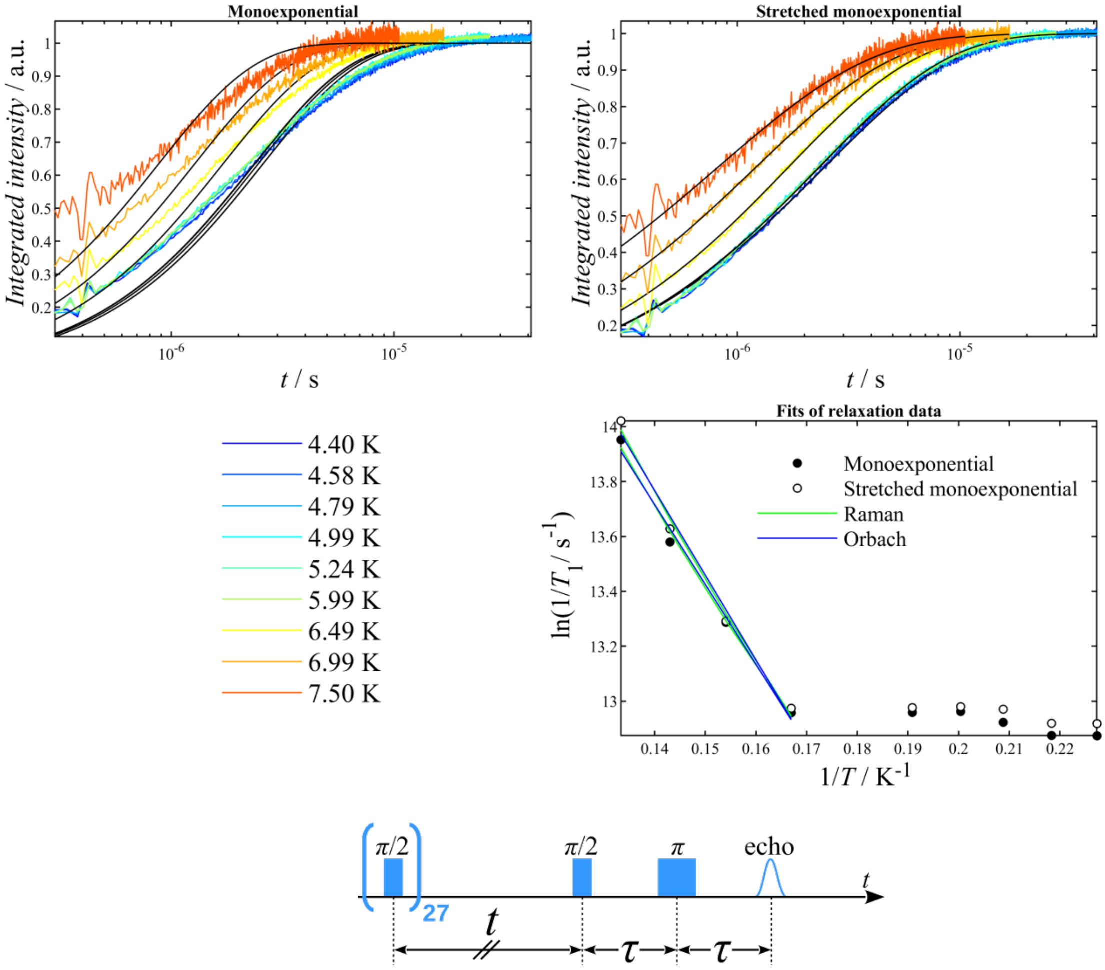

Figure S2. Variable-temperature saturation recovery data of **Cr$_3$** (colored lines) and fits to monoexponential (top left) and stretched exponential (top right) laws (black lines). The derived T_1 times are plotted as $1/T_1$ vs $1/T$ (bottom right) and the high-T regimes are fitted to Orbach and Raman processes. The pulse sequence is shown at the bottom.

Table S1. Best-fit parameters of variable-temperature saturation recovery traces of **Fe$_3$** and **Cr$_3$** to monoexponetial and stretched exponential laws.

	Fe$_3$		
	Monoexp.	**Stretched**	
T (K)	T_1 (μs)	T_1 (μs)	β
4.13	348(4)	379(4)	0.657(6)
4.39	344(4)	375(3)	0.651(6)
4.99	369(15)	392(11)	0.64(1)
6.00	51(1)	55(1)	0.73(1)
6.20	41(1)	42.7(9)	0.72(1)
6.40	30(1)	30.0(7)	0.69(1)
6.60	21.7(9)	22.0(6)	0.66(1)
6.80	12.0(3)	13.2(4)	0.75(2)
7.00	8.8(3)	9.3(3)	0.74(2)
7.40	5.1(2)	5.2(2)	0.68(3)
8.00	1.86(9)	2.0(1)	0.62(3)

	Cr$_3$		
	Monoexp.	**Stretched**	
T (K)	T_1 (μs)	T_1 (μs)	β
4.40	2.57(1)	2.45(1)	0.722(1)
4.58	2.56(1)	2.45(1)	0.721(1)
4.79	2.44(1)	2.33(1)	0.735(1)
4.99	2.35(1)	2.308(9)	0.7340(1)
5.24	2.36(1)	2.316(6)	0.741(1)
5.99	2.36(1)	2.319(6)	0.741(1)
6.49	1.70(1)	1.689(7)	0.745(1)
6.99	1.270(9)	1.206(8)	0.689(3)
7.50	0.873(8)	0.81(1)	0.621(5)

1.3. Inversion recovery studies of Fe_3

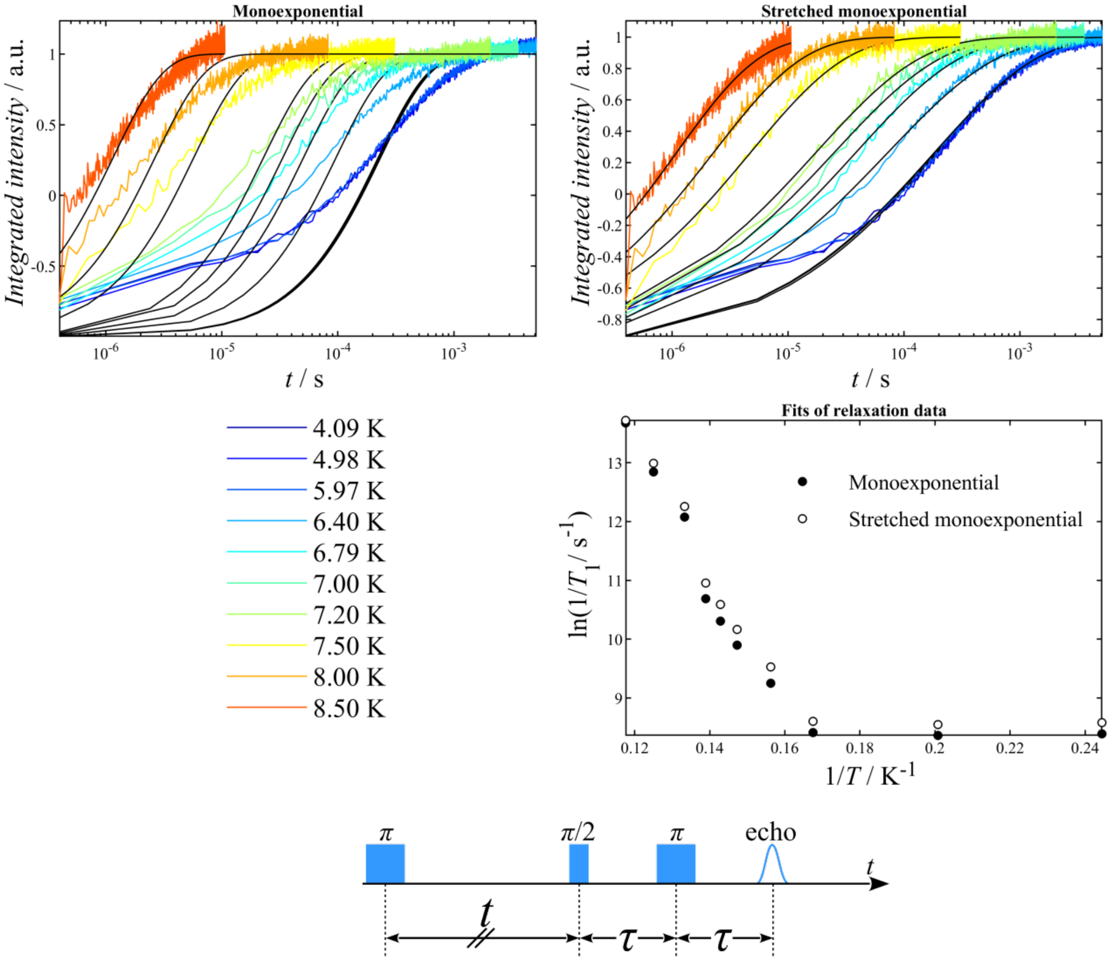

Figure S3. Variable-temperature inversion recovery data of **Fe_3** (colored lines) and fits to monoexponential (top left) and stretched exponential (top right) laws (black lines). The derived T_1 times are plotted as $1/T_1$ vs $1/T$ (bottom right). The pulse sequence is shown at the bottom.

1.4. Inversion recovery studies of Cr$_3$

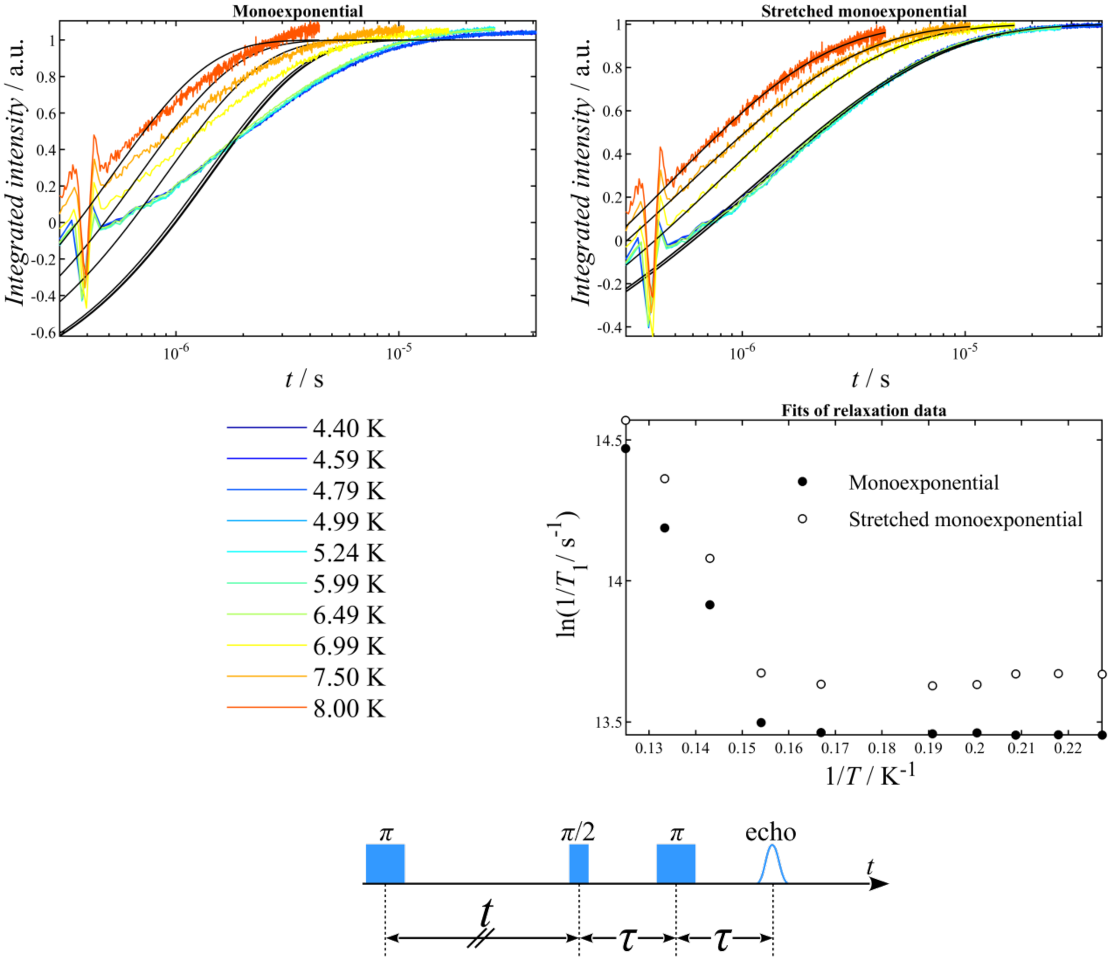

Figure S4. Variable-temperature inversion recovery data of **Cr$_3$** (colored lines) and fits to monoexponential (top left) and stretched exponential (top right) laws (black lines). The derived T_1 times are plotted as $1/T_1$ vs $1/T$ (bottom right). The pulse sequence is shown at the bottom.

2. Calculation of Debye temperature for the solid Fe_3

The Debye temperature for solid Fe_3 was calculated by fitting the previously reported[1] thermal dependence of its unit cell volume (Figure S 5) to the following equation:[2]

$$V(T) = V(0) + 3Nk_B\Theta'_D \frac{T}{\Theta_D}\mathrm{D}\left(\frac{\Theta_D}{T}\right) \quad \text{(S1)}$$

where N is the number of atoms per unit cell, $\Theta'_D = \frac{\mathrm{d}\Theta_D}{\mathrm{d}p}$ is the Debye temperature change as a function of pressure, and $\mathrm{D}(x) = \frac{3}{x^3}\int_0^x \frac{z^3}{e^z - 1}\mathrm{d}z$ is the Debye function. For $N = 274$ atoms, the best-fit results were $\Theta_{\mathrm{D}} = 199(24)$ K, $V_0 = 2933(1)$ Å^3, $k_B\Theta_D = 0.11(1)$ Å^3.

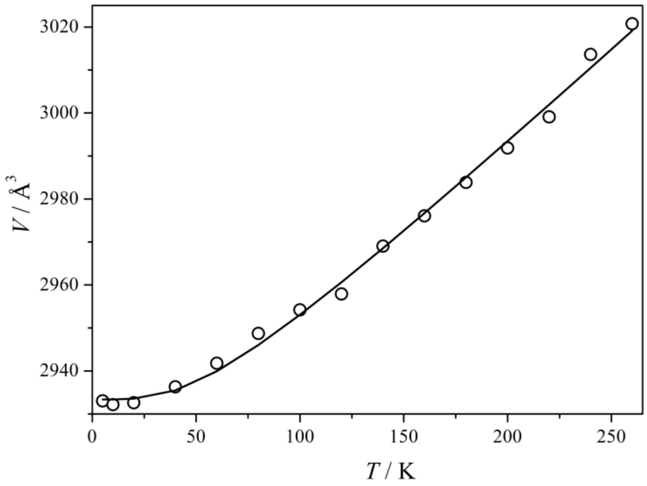

Figure S5. Variable-temperature unit-cell volume data and fit according to Equation S1.

The fits were carried out with a custom-made Matlab routine using a polylogarithm approximation of the Debye function:[3]

```
function y = Dpolylog(x)
y = x.*real((-1/5).*(pi^4)./power(x,4) - 3/4 +...
    3.*log(1 - exp(x))./x...
    +9.*polylog(2,exp(x))./power(x,2)...
    -18.*polylog(3,exp(x))./power(x,3)...
    +18.*polylog(4,exp(x))./power(x,4));
end
```

The arithmetical precision of this function was checked against an integral-based Matlab function implementing the Debye function definition:

```
function y = D(x)
fun = @(x) power(x,3)./(exp(x)-1);
y = 3./power(x,3) .* integral(fun,0,x);
end
```

The two were found to differ only after the tenth significant digit.

3. Spin-spin relaxation

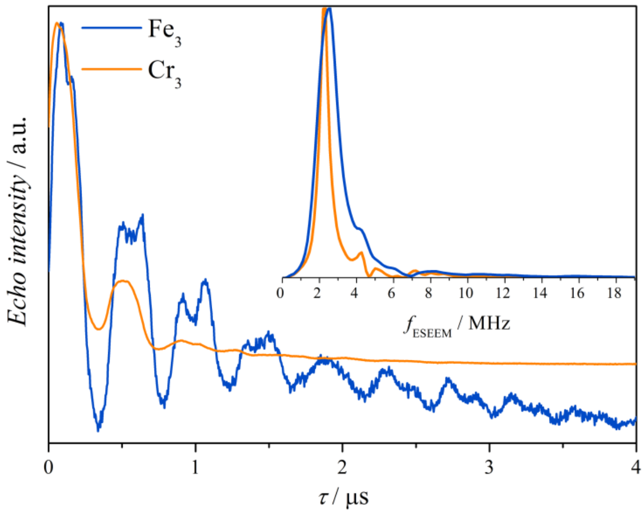

Figure S 6. Indicative Hahn echo decay traces (5.5 K) for **Fe₃** (red) and **Cr₃** (red). The inset shows the Fourier transforms of the decay curves.

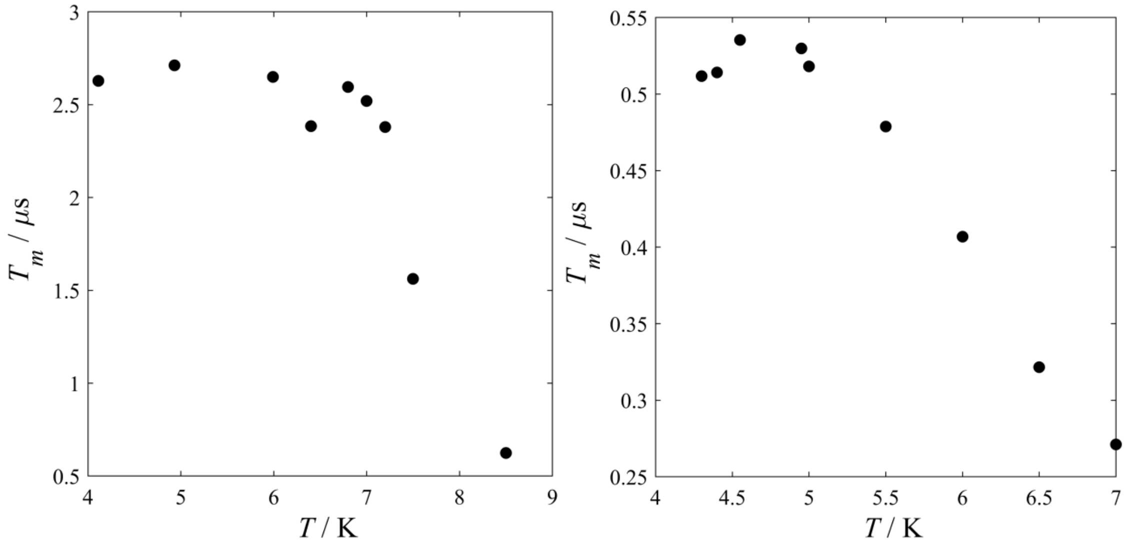

Figure S7. Thermal dependence of T_m times of **Fe₃** (left) and **Cr₃** (right) derived from fits to variable-temperature Hahn echo decay curves.

Table S2. Best-fit parameters of variable-temperature Hahn echo decay traces of **Fe_3** and **Cr_3** to the model described in the main text.

T (K)	T_m (μs)	f_{ESEEM} (MHZ)
4.11	2.6(1)	2.23(1)
4.93	2.7(1)	2.24(1)
5.99	2.7(1)	2.24(1)
6.40	2.4(1)	2.27(1)
6.80	2.6(1)	2.24(1)
7.00	2.5(1)	2.24(1)
7.20	2.4(1)	2.24(1)
7.50	1.56(5)	2.23(1)
8.50	0.62(2)	2.00(4)

T (K)	T_m (μs)	f_{ESEEM} (MHZ)
4.30	0.51(1)	2.30(1)
4.40	0.51(1)	2.30(1)
4.55	0.54(1)	2.28(1)
4.95	0.53(1)	2.28(1)
5.00	0.52(1)	2.28(1)
5.50	0.48(1)	2.30(1)
6.00	0.41(1)	2.36(2)
6.50	0.322(8)	2.36(3)
7.00	0.271(9)	2.48(5)

4. Nutation experiments

4.1. Fits to time domain experiments

The time-domain nutation traces were fitted to the following model:

$$\begin{aligned} &M_z(t_{nut}) = k_{R_1} e^{-t_{nut}/\tau_{R_1}} \cos(2\pi f_{R_1} t_{nut}) + \\ &+ k_{R_2} e^{-t_{nut}/\tau_{R_2}} \cos(2\pi f_{R_2} t_{nut} + \varphi_{R_2}) + \\ &+ k_H e^{-t_{nut}/\tau_{1_{\mathrm{H}}}} \cos(2\pi f_{1_{\mathrm{H}}} t_{nut} + \varphi_{1_{\mathrm{H}}}) \end{aligned} \tag{S2}$$

4.2. Frequency-domain nutation data

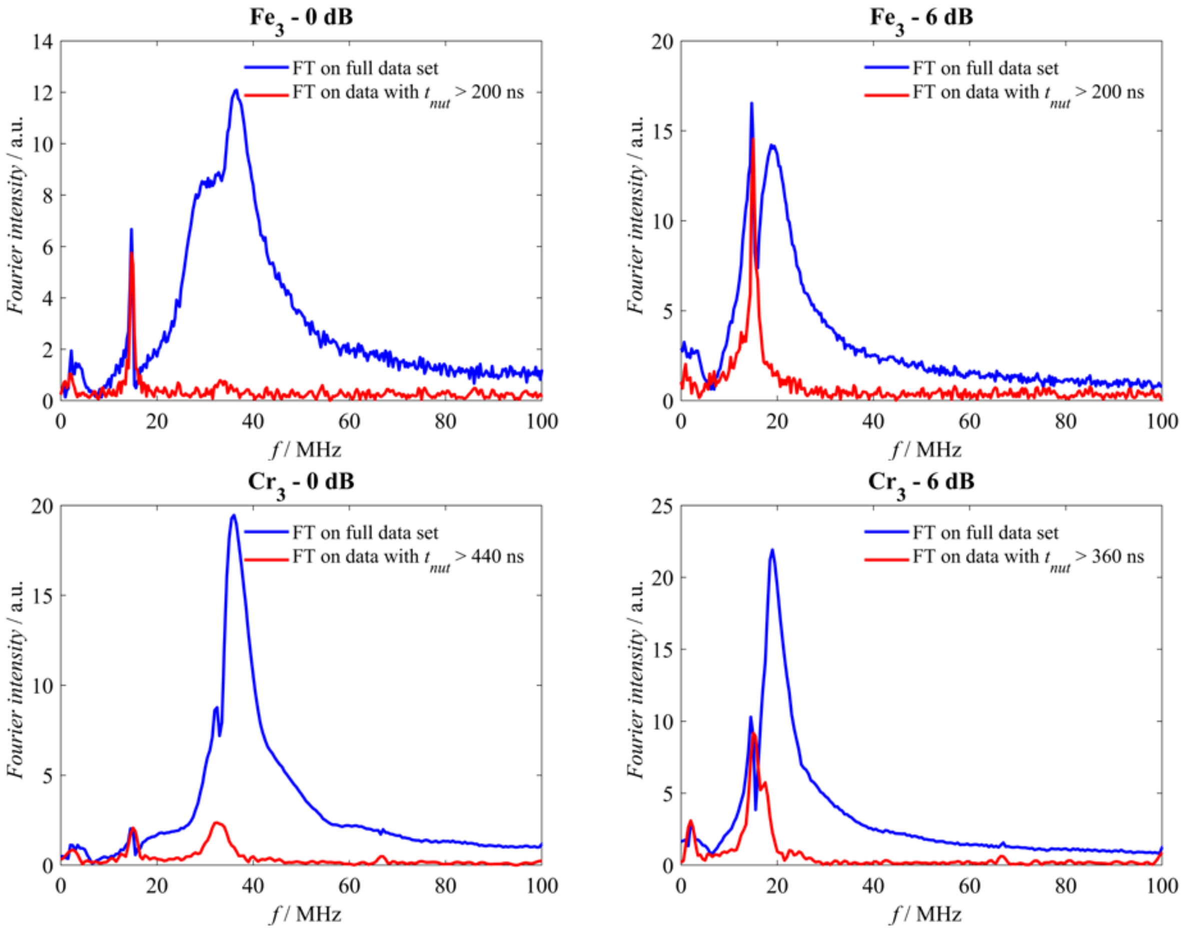

Figure S8. Fourier transforms of the full range of nutation data (blue lines) and of a partial data set chosen to start after the full damping of Rabi oscillations (red lines). The persistence of the longer-lived ESEEM peaks and the disappearance of the shorter-lived nutation peaks clearly distinguishes the different damping profiles of the two. The nutation of **Cr_3** is longer-lived than that of **Fe_3** and the peak suppression is not complete.

5. References

1 A. N. Georgopoulou, I. Margiolaki, V. Psycharis and A. K. Boudalis, *Inorg. Chem.*, 2017, **56**, 762–772.

2 H.-Y. Ko, R. A. DiStasio, B. Santra and R. Car, *Phys. Rev. Mater.*, 2018, **2**, 055603.

3 A. E. Dubinov and A. A. Dubinova, *Tech. Phys. Lett.*, 2008, **34**, 999–1001.